

Atomic scale characterization of HfO₂/Al₂O₃ Thin Films Grown on Nitrated and Oxidized Si Substrates

**T. Nishimura¹⁾, T. Okazawa¹⁾, Y. Hoshino¹⁾, Y. Kido¹⁾,
K. Iwamoto²⁾, K. Tominaga²⁾, T. Nabatame²⁾, T. Yasuda³⁾,
and A. Toriumi⁴⁾**

Abstract

One and three bilayers of HfO₂(9 Å)/Al₂O₃(3 Å) thin films were grown by atomic layer chemical vapor deposition on Si(001) substrates whose surfaces were nitrated or oxidized. The films as-grown and postannealed in an ultrahigh vacuum were analyzed by atomic force microscopy, photoelectron spectroscopy, and medium energy ion scattering. For the one- and three-bilayer films grown on the nitrated Si substrates, the HfO₂ and Al₂O₃ layers are mixed to form Hf aluminates at temperatures above 600 °C. The mixed Hf-aluminate layer is partly decomposed into HfO₂ and Al₂O₃ grains and Al₂O₃ segregates to the surface by postannealing at 900 °C. Complete decomposition takes place at 1000 °C and the surface is covered with Al₂O₃. The surfaces are uniform and almost flat up to 900 °C but are considerably roughened at 1000°C due to the complete decomposition of the Hf aluminate layer. In contrast, for one- bilayer films stacked on the oxidized Si substrates, Hf silicate layers, including Hf aluminates are formed by annealing at 600-800 °C. At temperatures above 900 °C, HfSi₂ grows and Al oxide escapes from the surface.

¹⁾ Department of Physics, Ritsumeikan University, Kusatsu, Shiga-ken 525-8577, Japan

²⁾ MIRAI Project, Association of Super-Advanced Electronics Technology (ASET), 16-1 Onogawa, Tsukuba, Ibaraki 305-8569, Japan

³⁾ MIRAI Project, Advanced Semiconductor Research Center, National Institute of Advanced Industrial Science and Technology (ASRC, AIST), 16-1 Onogawa, Tsukuba, Ibaraki 305-8569, Japan

⁴⁾ Department of Materials Science, Graduate School of Engineering, The University of Tokyo, 7-3-1 Hongo, Tokyo 113-8586, Japan, and MIRAI project, AIST, Japan

I. INTRODUCTION

High- k dielectrics are being considered as possible replacements for SiO₂ of the gate oxide of the complementary metal-oxide semiconductor (CMOS) devices, because the conventional oxide thickness is reduced into a regime in which direct tunneling current dominates the gate leakage current. Hafnium oxide (HfO₂) is the most promising candidate due to its high dielectric constant, wide band gap, and thermal stability in contact with Si substrates. It is needed, however, that the gate oxide films remain amorphous throughout the CMOS processing to suppress electric and mass transport along the grain boundaries. Unfortunately, the HfO₂ films formed by chemical-vapor deposition are crystalline¹ and postannealing accelerates the growth of definite grain boundaries.² In addition, HfO₂ is not effective against oxygen diffusion and, thus, SiO₂-rich interfacial layers are formed. To overcome this problem, some attempts have been made such as nitrogen and silicon introduction into HfO₂ films.^{3,4} Al₂O₃ is known to act as an oxygen diffusion barrier and also as a good glass former. It is recently reported that Hf aluminate films are thermally stable and remain amorphous up to 900 °C.⁵⁻⁷ The design of the interface structures that contains SiO₂, SiON, and SiN_x is also a key issue to control electrical properties. Very recently, Cho *et al.* reported the change of the chemical structure for HfAlO_x on oxidized Si substrates by annealing.⁸ However, the difference of the physical and chemical structure between HfAlO_x grown on nitrated and oxidized Si-substrates after annealing is not understood well.

In this study, we analyzed one and three bilayers of HfO₂(9 Å)/Al₂O₃(3 Å) films grown by atomic layer deposition (ALD) on nitrated and oxidized Si(001) substrates using high-resolution medium energy ion scattering (MEIS) and photoelectron spectroscopy (PES). The MEIS determined the elemental depth profiles and PES provided information on the electronic structure, such as chemical bonds, for the above samples as-grown and annealed at higher temperatures. An atomic force microscope (AFM) observed the surface morphology before and after annealing.

II. EXPERIMENT

The samples prepared are one and three bilayers of HfO₂(9 Å)/Al₂O₃(3 Å) thin films grown by ALD on p-type Si(001) substrates (resistivity: 1-5 Ω cm). The films were stacked at 250 °C on the nitrated (SiN_x: 7 Å) and oxidized (SiO₂: 14 Å) Si(001) substrates. One bilayer was formed by three ALD cycles for Al₂O₃ followed by nine ALD cycles for HfO₂ using Al(CH₃)₃ and Hf[N(CH₃)₂]₄, respectively. The layer thickness per each cycle was estimated to be about 1 Å. Postannealing was performed at temperatures from 500 to 1000 °C for 30 s by infrared radiation heating in an ultrahigh vacuum (UHV). The postannealed samples were analyzed *in situ* by MEIS and PES using synchrotron radiation (SR). Prior to MEIS measurement, all the samples were preannealed at 450 °C for 20 min in an UHV to eliminate a surface contamination.

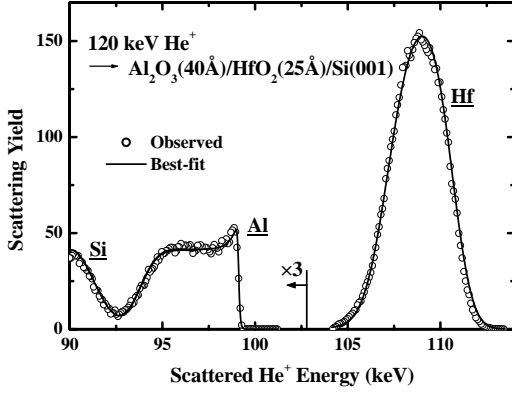


FIG. 1. MEIS spectra observed (circles) and best-fitted (solid curves) for 120 keV He^+ ions backscattered from $\text{Al}_2\text{O}_3(40\text{\AA})/\text{HfO}_2(25\text{\AA})/\text{Si}(001)$. The small surface peak seen for the scattering component from Al is generated by a non-equilibrium charge exchange process⁹.

In order to determine the depth profiles precisely, we prepared a standard sample of a thick $\text{Al}_2\text{O}_3/\text{HfO}_2$ stacked on the $\text{Si}(001)$ substrate, whose surface was oxidized. The absolute amount of HfO_2 was determined to be 25\AA (2.1×10^{16} atoms/cm²) by Rutherford backscattering using 2.0-MeV He^+ beams. Then, we measured the MEIS spectrum for the above standard sample using 120-keV He^+ ions, as shown in Fig. 1. The scattering yield

from some composite element is expressed by

$$Y_+ = Q(d\sigma/d\Omega)\Delta\Omega(N\Delta x)\eta_+\varepsilon, \quad (1)$$

where Q , $d\sigma/d\Omega$, $\Delta\Omega$, and $N\Delta x$ are the number of incident ions, differential scattering cross section, solid angle subtended by a detector, and areal density of the target atoms of interest, respectively. The fraction of He^+ is denoted by η_+ and ε is the detection efficiency of a toroidal spectrometer, which was determined to be 0.52 ± 0.03 in advance.¹⁰ The scattering cross sections were calculated from the Ziegler-Biersack-Littmark potentials,¹¹ taking account for the screening effects. The number of incident He^+ ions Q is known by measuring the integrated beam current precisely. From the best-fitting condition for the Hf spectrum, we obtain the stopping power of HfO_2 , He^+ fraction for the He ions scattered from Hf, and energy straggling for HfO_2 and Al_2O_3 . The stopping power value determined here is 1.1 times as large as that given by Ziegler¹¹ and the energy straggling for HfO_2 and Al_2O_3 are estimated to be $0.63\Omega_B$ and $0.54\Omega_B$ (Ω_B : Bohr straggling), respectively. The He^+ fractions are 0.50 and 0.46 for the He ions scattered from Hf and Al, respectively. The difference reflects the energy-dependent He^+ fraction. It is impossible to determine the absolute amount of Al and the stopping power of Al_2O_3 independently. So, we assumed that the stopping power of Al_2O_3 is also 1.1 times Ziegler's stopping power and obtained the Al_2O_3 thickness of 39\AA , which is compatible with the thickness ($40 \pm 10\text{\AA}$) measured by Rutherford backscattering spectroscopy (RBS) with 2.0-MeV He^+ beams. In the above discussion, the stoichiometry of HfO_2 and Al_2O_3 was assumed and the density of HfO_2 and Al_2O_3 was assumed to be 9.6 and 4.0 g/cm^3 , respectively. The real density of the above thin films would be significantly smaller than that of the bulk. However, to estimate the real density of the films, we have to compare the MEIS result [areal density (atoms/cm²)] with the image of the high-resolution transmission electron microscopy.

We observed *ex situ* the Al $2p$, Si $2p$, C $1s$, N $1s$, and Hf $4f$ core-level spectra together with the valence-band spectra using a monochromatic Al $K\alpha$ x ray (1486.6 eV). All the above spectra except for Si $2p$ were referenced to C $1s$ at 285.5 eV considering a surface charging effect. In the case of Si $2p$, the Si $2p$ binding-energy shifts were scaled from the bulk Si $2p_{3/2}$. The PES measurements with SR lights at photon energies of 40, 140, and 280 eV were also carried out. However, such low-energy photon beams are very surface sensitive and, thus, are not so suitable for the present interface analysis. In order to probe the surface morphology, we employed an AFM operating in a tapping mode.

III. RESULTS AND DISCUSSION

A. Growth on the nitrated Si substrates

Figure 2 shows the MEIS spectra for 120 keV-He⁺ ions scattered from HfO₂/Al₂O₃/SiN_x/Si as-grown (a) and postannealed at 900 °C (c). The solid curves are the simulated spectra best fitted to the observed ones assuming the elemental depth distributions indicated in the lower figures [Figs. 2(b) and 2(d)]. The thickness of the HfO₂ and Al₂O₃ layers is determined to be 8.5 and 1.9 Å, respectively. Here, to determine the Al₂O₃ thickness, we exploited the ratio of

the Al $2p$ to Hf $4f$ photoelectron intensities measured with the Al $K\alpha$ x ray. The above Al₂O₃ thickness is considerably smaller than that expected. This result indicates a low deposition rate on the nitrated surface at the initial stage (a few monolayers) of the ALD process. The present MEIS analysis reveals that mixing of HfO₂ and Al₂O₃ occurs for both the as-grown and postannealed samples. For the as-grown sample, about a half of Al₂O₃ is moved into the

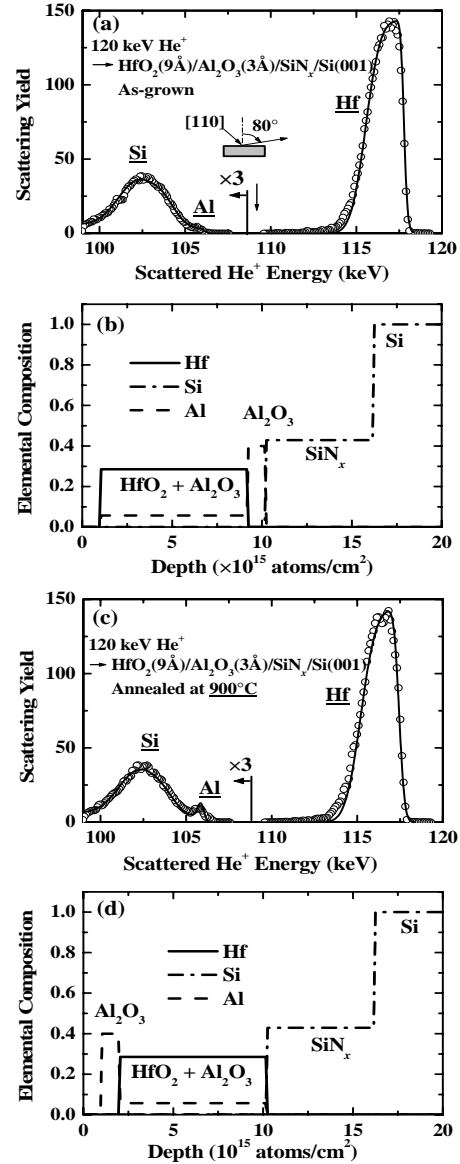


FIG. 2. MEIS spectra from HfO₂/Al₂O₃/SiN_x/Si as-grown (a) and post-annealed at 900 °C (c). 120 keV He⁺ ions are incident along Si-[101] axis and backscattered to 55°. Solid curves are best-fitted spectra assuming depth profiles indicated in the lower figures. About one monolayer of surface contamination (mainly carbon) still exists after pre-annealing at 450 °C in UHV.

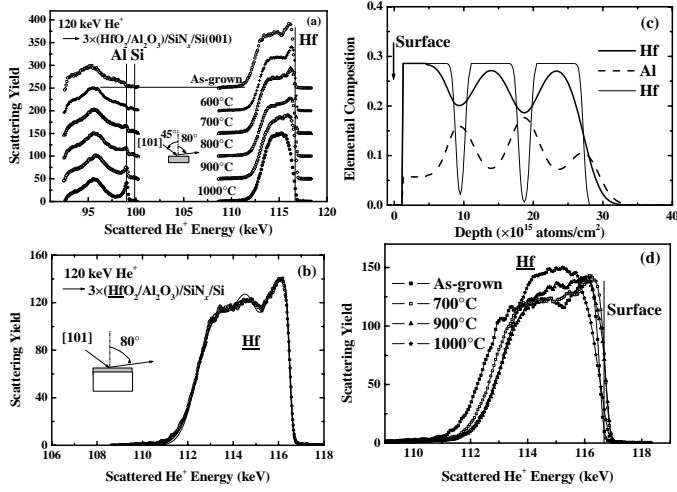


FIG. 3. (a) MEIS spectra observed with for the three bilayers films, $3 \times (\text{HfO}_2(9\text{\AA})/\text{Al}_2\text{O}_3(3\text{\AA}))/\text{SiN}_x(7\text{\AA})/\text{Si}(001)$ as-grown and post-annealed. 120 keV He^+ ions were incident along the [101]-axis and backscattered to 55° . The straight bars indicate the front edges for the Hf, Si, and Al. (b) MEIS spectra from Hf of the as-grown sample observed (circles) and simulated (thin and thick curve). Thick curve is the best-fitted spectrum assuming the elemental depth distributions (thick curve) indicated in Fig. (c). (d) Magnified MEIS spectra from Hf of the as-grown and post-annealed samples. The straight bar indicates the front edge of Hf corresponding to the energy position for the He^+ ions scattered from the Hf atoms located on the top surface.

thermally stable and suppresses the Si diffusion from the Si substrate to the high- k film up to 1000 °C.

Figure 3(a) shows the observed MEIS spectra for the three-bilayer films grown on the nitrided Si substrates as-grown and postannealed at 600 up to 1000 °C. A surface segregation of Al_2O_3 is seen for the samples postannealed at temperatures above 900 °C. The MEIS spectrum from Hf for the as-grown sample is shown in Fig. 3(b). The thick and thin solid curves are the simulated spectra assuming the elemental depth distributions indicated in Fig. 3(c). The best-fitting condition (thick solid curve) determines the total thickness of HfO_2 and Al_2O_3 to be 24 and 7 Å, respectively, which are comparable with the expected values. It is also found that the HfO_2 and Al_2O_3 layers are significantly interdiffused, probably due to preannealing at 450 °C. Figure 3(d) shows the magnified MEIS spectra from Hf for the samples as-grown and postannealed at 700, 900, and 1000 °C. The straight line indicates the front edge of Hf corresponding to the energy position for the He ions scattered from the Hf atoms on the top surface. It is seen that about one monolayer surface contamination still exists after preannealing at 450 °C and is eliminated by postannealing at 700 °C. The mixing of HfO_2 and Al_2O_3 proceeds to form a Hf aluminate by postannealing at 700 °C, and the mixed layer is partly decomposed into HfO_2 and Al_2O_3 grains by postannealing at 900 °C. Postannealing at 1000 °C leads to the complete

HfO_2 layer and the rest still exists on the SiN_x layer. Such a mixing may take place by preannealing at 450 °C for 20 min in an UHV immediately before the MEIS measurement. On the other hand, about a half of Al_2O_3 moves to the surface through the HfO_2 layer and the rest is incorporated in the HfO_2 layer for the sample postannealed at 900 °C. The MEIS analysis also reveals the fact that the SiN_x layer is almost

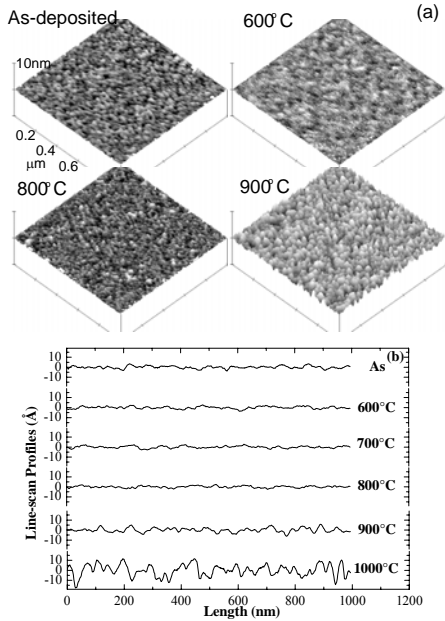


FIG. 4. AFM images (a) and the line-scans (b) for the as-grown and post-annealed samples.

and that of Al seems almost constant. This phenomenon at 1000 °C is quite different from what happened for the $\text{HfO}_2/\text{SiO}_2/\text{Si}$ system.¹²

We observed the Al $2p$, Si $2p$, C $1s$, N $1s$, and Hf $4f$ core-level spectra with the Al $K\alpha$ x-ray. Figure 5 shows the Si $2p$ spectra observed for the samples as-grown and postannealed at 600, 700, 800, 900, and 1000 °C. The spectra consist of two components from the bulk Si^0 and from silicon nitride. The Si $2p$ binding energy of the latter is higher, about 2.7 eV, than that of the former.¹³ It is consistent with the

previous MEIS result that the SiN_x layers are almost thermally stable and remain underneath the high- k films up to 1000 °C. The increase in the N $1s$ intensity was also observed by postannealing above 700 °C. This indicates that the SiN_x layer is partly decomposed and a part of nitrogen diffuses to the surface. For the samples postannealed at 600-900 °C, higher binding-energy shifts of about 0.2 eV, indicating the formation of Hf aluminates, were observed for Hf $4f$ (Fig. 6). The higher binding-energy shifts are responsible for the electronegativity of Hf (1.23) being lower than that of Al (1.47). The present result is consistent with that reported by Yu *et al.*¹⁴ After annealing at 1000 °C, the binding energy

decomposition of the Hf aluminate grains and the surface is covered completely with Al_2O_3 domains. The surface component is Al_2O_3 , not metallic aluminum, which was confirmed by the Al $2p$ core-level analysis using SR light.

Figure 4 shows the surface morphology observed by AFM (a) and the resultant line-scan profiles (b). It is clearly seen that the surfaces are uniform and almost flat for the samples postannealed at temperatures up to 800 °C. In fact, the rms of the surface height is ± 2 Å at most. By postannealing at 900 °C, the surface is slightly roughened, and postannealing at 1000 °C leads to a considerably roughened surface. Such surface roughening comes from the decomposition of the Hf aluminate layer into HfO_2 and Al_2O_3 domains. Here, it must be noted that the absolute amount of Hf is constant

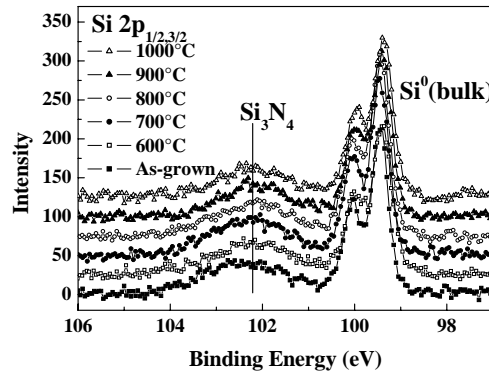


FIG. 5. Si $2p$ spectra observed by Al- $K\alpha$ for the as-grown and post-annealed samples. The binding energy is scaled by taking bulk Si $2p_{3/2}$ as a basis. From the bottom to the upper, the six spectra correspond to the samples as-grown, annealed at 600, 700, 800, 900, and 1000 °C.

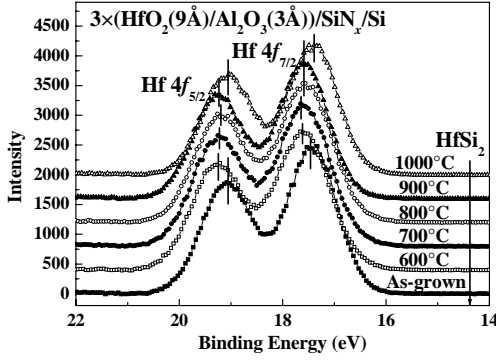


FIG. 6. Hf 4f spectra measured with Al $K\alpha$ for $3\times(\text{HfO}_2(9\text{\AA})/\text{Al}_2\text{O}_3(3\text{\AA}))/\text{SiN}_x/\text{Si}(001)$ as-grown and post-annealed at 600 - 1000 °C.

Figure 7 shows the MEIS spectra from one bilayer of $\text{HfO}_2(9\text{\AA})/\text{Al}_2\text{O}_3(3\text{\AA})/\text{SiO}_2(14\text{\AA})/\text{Si}$ as-grown (a) and postannealed at 800 °C (c). It is seen that mixing of HfO_2 and Al_2O_3 occurs for both samples. However, for the sample annealed at 800 °C, Si atoms are diffused into the mixed layer to form a Hf silicate plus an Al_2O_3 and/or a Hf aluminate layer. The AFM observation showed a relatively uniform surface with a roughness of $\pm 2\text{-}3\text{\AA}$. The formation of the Hf silicate leads to a lowered and slightly broadened spectrum from Hf and to an increase in the spectrum height from Si in the surface region. The mixing seen for the as-grown sample is probably due to preannealing at 450 °C. In contrast to the nitrified Si substrates, no surface segregation of Al_2O_3 takes place for the oxidized Si substrates. The silicate formation occurs at temperatures above 600 °C. It is confirmed by the Si $2p$ core-level shifts, as shown in Figs. 8(a) and 8 (b). The binding-energy shift (ΔE) is scaled from the bulk $\text{Si}^0 2p_{3/2}$. The lower binding energy shifts for the samples annealed at temperatures above 600 °C suggests the formation of Hf silicates. For a poly-Si/ $\text{HfO}_2/\text{SiO}_2/\text{Si}$ system, Wilk and Muller¹⁵ observed a well-ordered HfO_2 microstructure and no Hf silicate layer at either interface on a scale down to 2 Å at temperatures above 600 °C. This suggests that SiO_2 is not incorporated into the crystallized HfO_2 at temperatures above 600 °C but could be incorporated into an amorphous Hf aluminate layer. In the previous study, we obtained a relation between the Si $2p_{3/2}$ binding-energy shift for Hf silicates as a function of the Hf

returns to that for the as-grown sample. It corresponds to the complete decomposition of Hf aluminate into HfO_2 and Al_2O_3 grains. In the case of the Al $2p$ spectra, the binding energy observed for the samples annealed at 600-1000 °C are almost the same within experimental uncertainties, probably due to insufficient statistics.

B. Growth on oxidized Si substrates

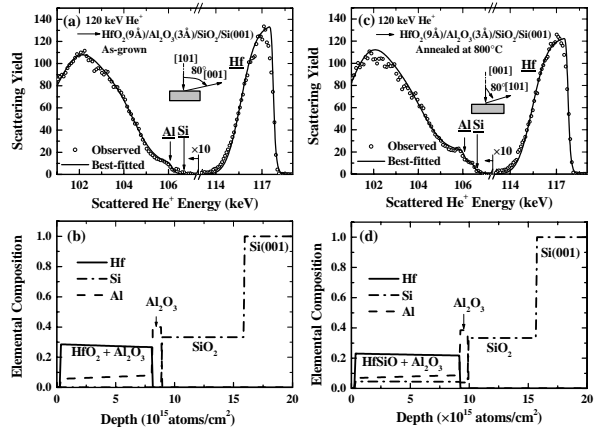


FIG. 7. MEIS spectra observed for 120 keV He^+ ions scattered to 55° from $\text{HfO}_2(9\text{\AA})/\text{Al}_2\text{O}_3(3\text{\AA})/\text{SiO}_2(14\text{\AA})/\text{Si}(001)$ as-grown(a) and post-annealed at 800°C(c). Solid curves are best-fitted spectra assuming depth profiles indicated in the lower figures.

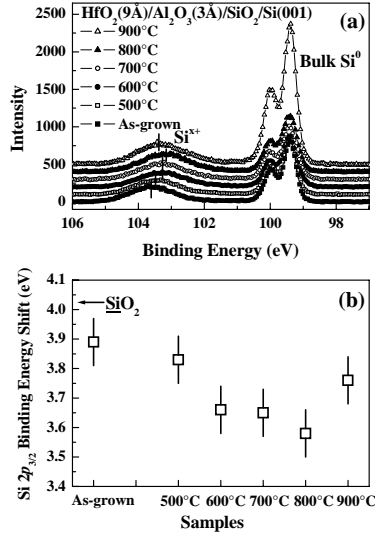


FIG. 8. (a) Si 2p spectra observed with Al-K α for HfO₂(9Å)/Al₂O₃(3Å)/SiO₂(14Å)/ Si(001) as-grown and post-annealed at 500-900°C. From the bottom to the upper, the six spectra correspond to the samples as-grown, annealed at 500, 600, 700, 800, and 900°C. (b) Si 2p_{3/2} binding energy shifts scaled by taking bulk Si⁰ 2p_{3/2} as a basis.

we prepared the standard sample of HfSi₂, which was formed by postannealing Hf(500 Å)/Si(001) at 800 °C in an UHV. Its elemental composition was determined to be Hf/Si = 1/2 by RBS with 2.0 MeV He⁺ ions. The observed Hf 4f peak for the sample annealed at 900 °C coincides well with that for the HfSi₂ standard. It is reported recently that such silicidation takes place for HfO₂/SiO₂/Si system at temperatures above 900 °C,¹⁷ and its formation rate is strongly dependent of the HfO₂ overlayer thickness.¹² The Al 2p spectra were also observed with the Al K α x ray but no binding-energy shifts were seen for the samples as-grown and annealed at 500-800 °C. It suggests the formation of Hf silicate rather than Hf-Al silicate for annealing at 600-800 °C. By annealing at 900 °C, however, the Al 2p peak disappears, indicating the escape of Al oxide from the surface. Recently, Kundu *et al.*¹⁸ investigated the thermal stability of ultrathin Al₂O₃ films on Si(001) and found a dissipation of Al₂O₃ by postannealing at 900 °C in an UHV and suggested the following reaction; Al₂O₃ (solid) + 2Si (solid) → Al₂O (gas) + 2SiO (gas). Such a reaction probably happened for the present HfO₂(9 Å)/Al₂O₃(3 Å)/SiO₂/Si(001) sample annealed at 900 °C in an UHV.

concentration.¹⁶ According to this relation, the ΔE value of 3.6 eV correspond to the Hf concentration of 40 at. %. Thus, postannealing at temperature in the range of 600 – 800 °C leads to the formation of Hf silicates with the Hf/(Hf + Si) ratio ranging from 35 % to 40 %. The present MEIS result shows that the Hf/(Hf + Si) ratio is about twice as that predicted by the Si 2p core-level shift. The disagreement suggests formation of Hf aluminate.

Figure 9 shows the Hf 4f spectra observed with the Al K α x rays. Also, in this case, the higher the annealing temperature, the higher the binding-energy shift for the samples annealed at 600 – 800 °C. This also means the formation of Hf silicate because the electronegativity of Hf (1.23) is considerably lower than that of Si (1.8). As clearly seen, postannealing at 900 °C generates HfSi₂. We

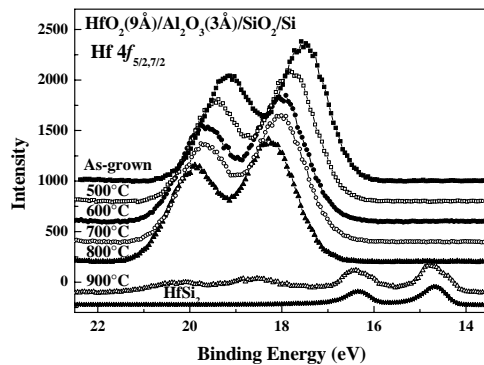


FIG. 9. Hf 4f_{5/2,7/2} spectra from HfO₂(9Å)/Al₂O₃(3Å)/SiO₂(14Å)/Si(001) as-grown and post-annealed at 500-900°C and from HfSi₂ standard.

IV. CONCLUSION

One and three bilayers of $\text{HfO}_2(9 \text{ \AA})/\text{Al}_2\text{O}_3(3 \text{ \AA})$ thin films were stacked by ALD on the nitrided and oxidized Si(001) substrates. The films as-grown and postannealed at 500-1000 °C in an UHV were analyzed by AFM, PES, and MEIS. For the one- and three-bilayer films grown on the nitrided Si substrates, the HfO_2 and Al_2O_3 layers are mixed to form Hf aluminates at temperatures above 600 °C. The mixed Hf aluminate layer is partly decomposed into HfO_2 and Al_2O_3 grains and the Al_2O_3 segregates to the surface by postannealing at 900 °C. A complete decomposition takes place at 1000 °C, and the surface is covered with Al_2O_3 . The surfaces are uniform and almost flat up to 900 °C but are considerably roughened at 1000 °C due to the complete decomposition of the Hf aluminate layer. It is also found that the SiN_x buffer layer is almost thermally stable and still exists at temperatures up to 1000 °C. In contrast, for one-bilayer films stacked on the oxidized Si substrates, Hf silicate layers incorporating Hf aluminate are formed by annealing at temperatures in the range of 600 – 800 °C. At temperatures above 900 °C HfSi_2 grows and Al oxide escapes from the surface.

Acknowledgments

The authors would like to thank Dr T. Ishida for kindly allowing the use of the PES equipment. Special thanks are also due to Mr. A. Tsuda for his support on the MEIS analysis. This work was partly supported by NEDO.

References

1. M.-Y. Ho *et al.*, J. Appl. Phys. **93**, 1477 (2003).
2. Y. Harada, M. Niwa, S. Lee, and D.-L. Kwong, Digest of Technical Papers, Proceedings of the 2002 Symposium on Very Large Scale Integration (VLSI) Technology, Honolulu, Hawaii, 11-13 June 2002 (IEEE, New York, 2002), p. 26.
3. G.D. Wilk, R.M. Wallace, and J.M. Anthony, J. Appl. Phys. **87**, 484 (2000).
4. K. Onishi, C.S. Kang, R. Choi, H.-J. Cho, S. Gopalan, R.E. Nieh, S.A. Krishnan, and J.C. Lee, IEEE Trans. Electron Devices **50**, 384 (2003).
5. C.-W. Yang *et al.*, Electron. Lett. **38**, 1223 (2002).
6. M.-Y. Ho *et al.*, Appl. Phys. Lett. **81**, 4218 (2002).
7. P.F. Lee, J.Y. Dai, K.H. Wong, H.L.W. Chan, and C.L. Choy, Appl. Phys. Lett. **82**, 2419 (2003).
8. M.-H. Cho *et al.*, Appl. Phys. Lett. **84**, 571 (2004).
9. Y. Kido, T. Nishimura, and F. Fukumura, Phys. Rev. Lett. **82**, 3352 (1999).

10. Y. Kido, S. Semba, and Y. Hoshino, *Current Appl. Phys.* **3**, 3 (2003).
11. J.F. Ziegler, J.P. Biersack, and U. Littmark, *The Stopping and Range of Ions in Solids*, Pergamon, New York, 1985.
12. S. Sayan, E. Garfunkel, T. Nishimura, W.H. Schulte, T. Gustafsson, and G.D. Wilk, *J. Appl. Phys.* **94**, 928 (2003).
13. H.Y. Yu *et al.*, *Appl. Phys. Lett.* **81**, 376 (2002).
14. P.D. Kirsch, C.S. Kang, J. Lozano, J.C. Lee, and J.G. Ekerdt, *J. Appl. Phys.* **91**, 4353 (2002).
15. G.D. Wilk, and D.A. Muller, *Appl. Phys. Lett.* **83**, 3984 (2003)
16. Y. Hoshino, Y. Kido, K. Yamamoto, S. Hayashi, and M. Niwa, *Appl. Phys. Lett.* **81**, 2650 (2002).
17. N. Miyata, M. Ichikawa, T. Nabatame, T. Horikawa, and A. Toriumi, *Jpn. J. Appl. Phys.*, Part 2 **42**, L138 (2003).
18. M. Kundu, N. Miyata, and M. Ichikawa, *J. Appl. Phys.* **92**, 1914 (2002).